Water Science & Technology

IWA PUBLISHING

Water Science & Technology Vol 89 No 4, 859 doi: 10.2166/wst.2024.033

Battery waste-derived magnetic Fe–Mn–Zn/C composites as an electro-Fenton-like catalyst for the degradation of sodium dodecyl sulfate surfactant

Azhan Ahmad[a,*], Monali Priyadarshini[b], Makarand M. Ghangrekar[a] and Rao Y. Surampalli[c]

[a] Department of Civil Engineering, Indian Institute of Technology Kharagpur, Kharagpur 721302, India
[b] School of Environmental Science and Engineering, Indian Institute of Technology Kharagpur, Kharagpur 721302, India
[c] Global Institute for Energy, Environment and Sustainability, Kansas, USA
*Corresponding author. E-mail: azhan.ahmad246@gmail.com

ABSTRACT

A batch-scale electro-Fenton (EF) process was performed using graphite anode and waste battery-based Fe -Mn -Zn/C electrocatalyst coated on low-cost graphite felt cathode. The effectiveness of the EF's performance was evident with around 83.9 + 4.1% removal of 20 mg/L of sodium-dodecyl sulfate surfactant (SDS) at an optimum current density (CD) of 5.0 mA/cm^2, Na_2SO_4 of 0.05 M, initial pH of 7.2, and electrolysis time of 180 min. Moreover, nearly 1.78-fold more removal of SDS was achieved in EF than in the electro-oxidation process operated without any catalyst. The operating cost of 0.35 $ of per m^3 per order was needed to treat SDS wastewater. The remediation of SDS follows pseudo-first-order kinetics with a rate constant of 0.0095 min^{-1}. Additionally, 90.3 + 2.1% of SDS and 57 + 2.6% of total organic carbon (TOC) removal was attained during 240 min of treatment time in secondary treated real wastewater; hence, additional 60 min of treatment time is required for effectively treating real wastewater than synthetic wastewater. Thus, EF is effective with battery waste-derived magnetic catalyst for treating wastewater containing SDS, which can lead to achieving sustainable environmental goals.

Key words: battery waste, electro-Fenton, surfactant, waste management, wastewater treatment

HIGHLIGHTS

- The current work demonstrates a waste-to-treat-waste approach.
- Magnetic Fe–Mn–Zn/C catalyst derived from battery waste was used in electro-Fenton.
- Efficacious degradation of surfactant was obtained with a battery waste catalyst.
- The kinetics of removal obtained a pseudo-first-order kinetic model.
- Lauric acid was formed during sodium dodecyl sulfate degradation.

GRAPHICAL ABSTRACT

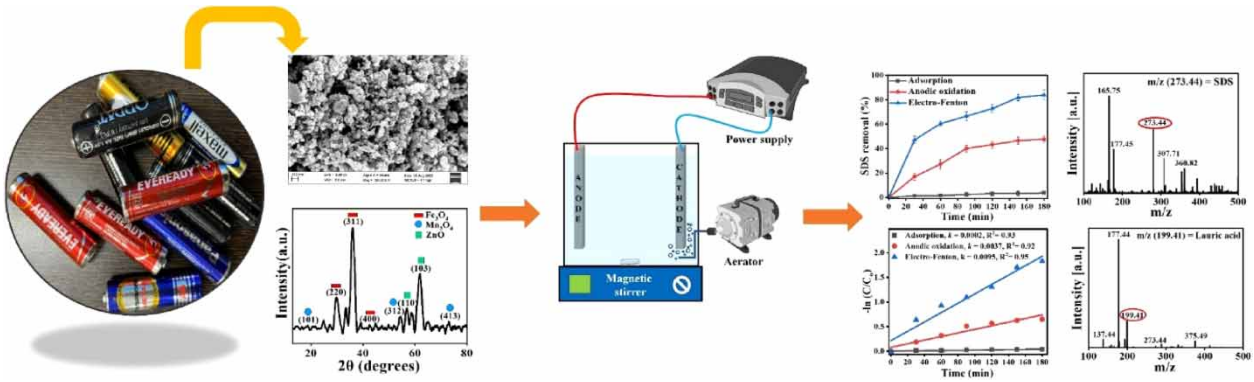

INTRODUCTION

The utilization of batteries in electronic devices has increased in the last three decades owing to their low cost and maintenance. For example, zinc-carbon batteries are frequently used in toys, remote controls, radios, and other electronic devices (Loudiki *et al.* 2022). However, after its usage, these batteries are incinerated or dumped into the landfill, which can pose an environmental risk due to the presence of metals present in it. Additionally, these batteries also contain manganese, zinc, iron, and carbon, which are basic elements used in the preparation of electrochemical catalysts (Arun *et al.* 2020; Wu *et al.* 2022). Iron can initiate the Fenton reaction, and carbon can improve the conductivity of the electrocatalyst for the degradation of organics from the wastewater (Gan *et al.* 2020). Moreover, the presence of other metals like zinc and manganese can improve the catalytic activity of iron and trigger the *in situ* production of hydrogen peroxide (H_2O_2) for the oxidation of complex organic pollutants (Yang *et al.* 2020; Fu *et al.* 2021). For instance, Ozturk utilized the Fe_3O_4/Mn_3O_4/ZnO-rGO for about 97% removal of chemical oxygen demand (COD) with an initial concentration of 3,560 mg/L via heterogeneous electro-Fenton (EF) process in about 79 min at a current density (CD) of 7.37 mA/cm^2 (Ozturk 2022). However, the catalyst was synthesized by using metal salts, which might not be economical during the real-scale implementation of the process for wastewater treatment. Thus, the utilization of battery waste for recycling metals in the form of catalysts can be a sustainable solution to tackle the environmental problems associated with waste management.

Besides, organic pollutants like sodium dodecyl sulfate (SDS) surfactant is frequently detected in sewage with a concentration ranging between 3 and 20 mg/L and can pose a risk to aquatic ecosystems (Saha *et al.* 2020). Also, the occurrence of SDS in water bodies can lead to foam formation; thereby deteriorating the water quality. Moreover, conventional treatment technologies are not efficacious in treating SDS-laden wastewater (Mondal *et al.* 2019). In this regard, the EF process, wherein *in situ* H_2O_2 is produced at the cathode (Equation (1)) by electrochemical reduction of oxygen along with catalytic Fe^{2+} supporting the generation of hydroxyl radical ($^{\bullet}OH$) in the system which is responsible for the oxidation of organic contaminants present in the solution (Equation (2)) (Priyadarshini *et al.* 2022):

$$O_2 + 2H^+ + 2e^- \rightarrow H_2O_2 \quad (1)$$

$$Fe^{2+} + H_2O_2 \rightarrow Fe^{3+} + {}^{\bullet}OH + OH^- \quad (2)$$

Previous work on SDS removal used tin-based zirconium and kaolin (SnZrK) catalyst and achieved 75% abatement of 20 mg/L of SDS via electro-oxidation (EO) process (Saha *et al.* 2020). However, the SnZrK catalyst was synthesized using chemical salts of tin and zirconium, which can incorporate the high cost of the catalyst and EO operation during field-scale application of SDS wastewater treatment. Similarly, Yuksel *et al.* reported 81.6% removal of 60 mg/L of SDS through the peroxi-electrocoagulation process (Yüksel *et al.* 2009). However, the external addition of H_2O_2 in the setup is the major limitation of the process due to its storage and transportation cost (Priyadarshini *et al.* 2022). On the other hand, our previous work demonstrated the effective abatement of pollutant salicylic acid by applying the waste iron-based-EF catalyst (Priyadarshini *et al.* 2023). Similarly, Ye and co-authors achieved efficacious degradation of Bisphenol A in EF with E-waste-derived Cu–Au catalyst (Ye *et al.* 2023).

Considering all these aspects, the current exploration, for the first time, employs the battery waste-derived magnetic Fe–Mn–Zn/C composites for the remediation of SDS from wastewater. In addition, the previous work on battery waste does not use all the components of the battery; herein, for the first time, the outer shell of the battery containing waste steel was also utilized for synthesizing the magnetic iron-based Fenton catalyst for its application in wastewater treatment. The present research work is based on the hypothesis that the battery waste containing iron, manganese, zinc, and carbon, converted into a cathode catalyst might be able to enhance the electrocatalytic activity of the Fe–Mn–Zn/C-based CF cathode. This can help in supporting the Fenton oxidation of the surfactant.

Thus, the objective of this investigation was to synthesize electrocatalysts from waste batteries for EF of SDS from wastewater. The physico and electrochemical properties of the as-synthesized catalyst were also elucidated. Different systems, such as adsorption, anodic oxidation, and EF pertaining to SDS using battery waste-based catalysts were elucidated. Moreover, the impact of operating factors like CD, initial pollutant dose, and anions, which affect the performance of the EF technique, has also been explored in the present demonstration. Also, the reusability of the battery waste catalyst for consecutive cycles was explored in terms of SDS removal. Besides, the dominant radicals responsible for EF of SDS have been investigated. Lastly,

the degradation pathway of SDS removal and economics of the system were also explored. Hence, the current demonstration can help in the management of waste along with the treatment of wastewater.

EXPERIMENTATION

Chemicals used

Analytical-grade SDS, hydrochloric acid (HCl), ammonium hydroxide (NH_4OH), sodium hydrogen carbonate ($NaHCO_3$), sodium chloride (NaCl), and sodium nitrate ($NaNO_3$) were procured from Sigma Aldrich, India. Ethanol (EtOH), benzoquinone (BQ), tert-butanol (TBA), and Bovine liver catalase (CAT, 11,700 U/mg) were procured from SRL, India.

Preparation of catalysts

The discharged old batteries were collected from IIT Kharagpur market (India) and manually dismantled. The outer cover of the battery containing iron as well as anodic metal containing zinc was separately digested in 1 M HCl (250 mL) for 24 h, and then the solution pH was raised to around 9.0 with 5 M NH_4OH to precipitate the iron and zinc metal (Chen *et al.* 2019; Setiadi *et al.* 2019). Besides, the inner material containing manganese and carbon powder was mixed in distilled water with an equal weight of iron and zinc powder obtained and subsequently oven-dried at 100 °C for 12 h. After that, the dried mixture was further oxidized at 350 °C in a muffle furnace for 1 h. Finally, the oxidized powder was again washed with distilled water repeatedly and oven-dried overnight to obtain Fe–Mn–Zn/C composites. The preparation of the catalyst is depicted in Supplementary material, Figure S1.

Electrode fabrication

The CF was pre-treated using acetone and distilled water before it was subjected to EF setup. The CF of size 5 cm × 3 cm × 0.5 cm was dipped in 40.0 mL of acetone for half an hour, then washed with distilled water and oven-dried for 300 min. Ink for CF was prepared using 2 mg/cm^2 of Fe–Mn–Zn/C composite catalysts, 20 mL of acetone, and 6.66 μL/mg of poly (dimethyl siloxane) binder following (Priyadarshini *et al.* 2023). Furthermore, the as-prepared ink solution was sonicated for 120 min for homogeneity and sprayed over a bare CF using air-brush spray. After achieving a uniform and consistent coating on the electrode surface, the electrode was subjected to oven drying for approximately 60 min.

Experimentation setup

The SDS abatement test was executed in a reactor (working volume = 350 mL) using an aqueous media of Na_2SO_4 (0.05 M) as an electrolyte (Supplementary material, Figure S2). The electrolyte was added to improve the conductivity of the synthetic wastewater for operating EF. Furthermore, the electrolyte solution was continuously oxygenated by an aquarium aerator for homogenous mixing, and an external current was supplied using a DC supply (1502 D-VAR Tech; current range = 0.1–0.3 A). Also, aeration during the experiment supports the H_2O_2 generation (Qi *et al.* 2022). For the anode, a graphite electrode was chosen; where the as-prepared electrode (Fe–Mn–Zn/C on CF) was used as a cathode for the EF experiment. Later, at regular time intervals, samples were collected and passed through 0.45 μm filter paper before analysis in a UV–vis spectrophotometer (T80, PG Instrument Ltd; $\lambda = 467$ nm) (Mondal *et al.* 2019).

All the experiments were performed in triplicates, and the corresponding standard deviation was calculated. Simultaneously, the H_2O_2 quantification was performed using a spectrophotometer at $\lambda = 570$ nm using the iodide method (Graf & Penniston 1980). Furthermore, the possible SDS degradation pathway and intermediates were detected using the matrix-assisted laser desorption ionization time-of-flight mass spectrometry (MALDI-TOF MS) analysis (Bruker ultrafleXtreme, Germany). Total organic carbon (TOC) analyzer was used to determine the TOC concentration during the SDS degradation in the EF process (Aurora 1030, USA). An automated digital meter was used to analyze the pH of the wastewater. The leaching of iron, zinc, and manganese in the treated wastewater was checked using ICP-MS (iCAP RQ, Thermo Scientific). The electron paramagnetic resonance (EPR) was performed to investigate the dominant radical species in the presence of 5,5-dimethylpyrroline-N-oxide (DMPO) as a trapping agent using pulsed EPR spectrometer (Bruker, ELEXSYS 580, Germany).

Physicochemical and electrochemical characterization of Fe–Mn–Zn/C composites

The crystal structure of the Fe–Mn–Zn/C catalyst was identified using an X-ray diffractometer having specifications D2 Phaser Bruker (USA), Cu Kα radiation, and $2\theta = 10$–80°. The Fourier transform infrared spectroscopy (FTIR, Bruker, Germany) was performed to identify the surface functionality and morphology of the catalyst. To reveal the microstructure

and surface topography, scanning electron microscopy (SEM; MERLIN, Zeiss) was performed; where the elemental abundance was estimated using electron dispersion X-ray spectroscopy (EDX; Oxford EDX detector, UK). The electrochemical characteristics like cyclic voltammetry (CV), linear sweep voltammetry (LSV), Tafel plots, and electrochemical impedance spectroscopy (EIS) were performed using a three-electrode based electrochemical workstation (Metrohm Autolab, Switzerland) in 0.05 M Na_2SO_4 electrolyte with a scan rate of 0.05 mV/s between potential range of –2.0 and +2.0 V.

RESULTS AND DISCUSSION

Physiochemical characteristics of the catalyst

The scanning electron microscope (SEM) of the electrocatalyst revealed the presence of distinct spherical particles of nanometer size (Figure 1(a)). Moreover, agglomerated spheres on a few tetrahedral structures were also visible in the SEM image. This can be due to the presence of zinc and iron spheres mounted on manganese to form a composite (Zavar 2017; Sathe *et al.* 2022). To further clarify the presence of metal particles in the composite catalyst, the energy-dispersive X-ray (EDX) was performed, which revealed the presence of Fe, Mn, Zn, and carbon (C) in the electrocatalyst (Figure 1(b)). In addition, the FTIR (Figure 1(c)) revealed a peak around 3,492 and 1,621 cm^{-1}, which was attributed to the stretching and deformation vibration of OH^- molecules on the surface of the electrocatalyst (Sathe *et al.* 2022). A few sharp clusters around 570 cm^{-1} were also observed, which can be due to the vibration of Mn – O or Zn – O of the catalyst (Subramani & Sathish 2019). In addition, an intense peak around 548 cm^{-1} was attained, revealing the bending vibration of Fe – O (Bashir *et al.* 2019). A peak assigned to the wavenumber of 1,079 and 1,360 cm^{-1} is ascribed to the stretching vibration mode of C–C and C–O, which might be present in the catalyst owing to the addition of graphite rod of the battery waste (Shi *et al.* 2010; Naseem *et al.* 2020).

Besides, the XRD analysis disclosed the formation of Fe_3O_4 corresponding to the sharp peak at 2θ of 30, 36, and 42.5° for planes 220, 311, and 400, respectively (JCPDS-86-1356) (Figure 1(d) (Priyadarshini *et al.* 2023). Also, peaks at 2θ of 18.9, 54, and 72.9° for planes 101, 312, and 413, respectively, revealed the formation of Mn_3O_4 (JCPDS-24-0734) (Ozturk 2022). Moreover, the hexagonal phase of ZnO was also formed in the catalyst, justified by the presence of peaks at 2θ of 56.8 and 62° for planes 110 and 103, respectively (JCPDS-89–0511) (Ozturk 2022). Hence, metal oxide composites were formed by battery waste, which can be further utilized as an electrocatalyst in the EF process.

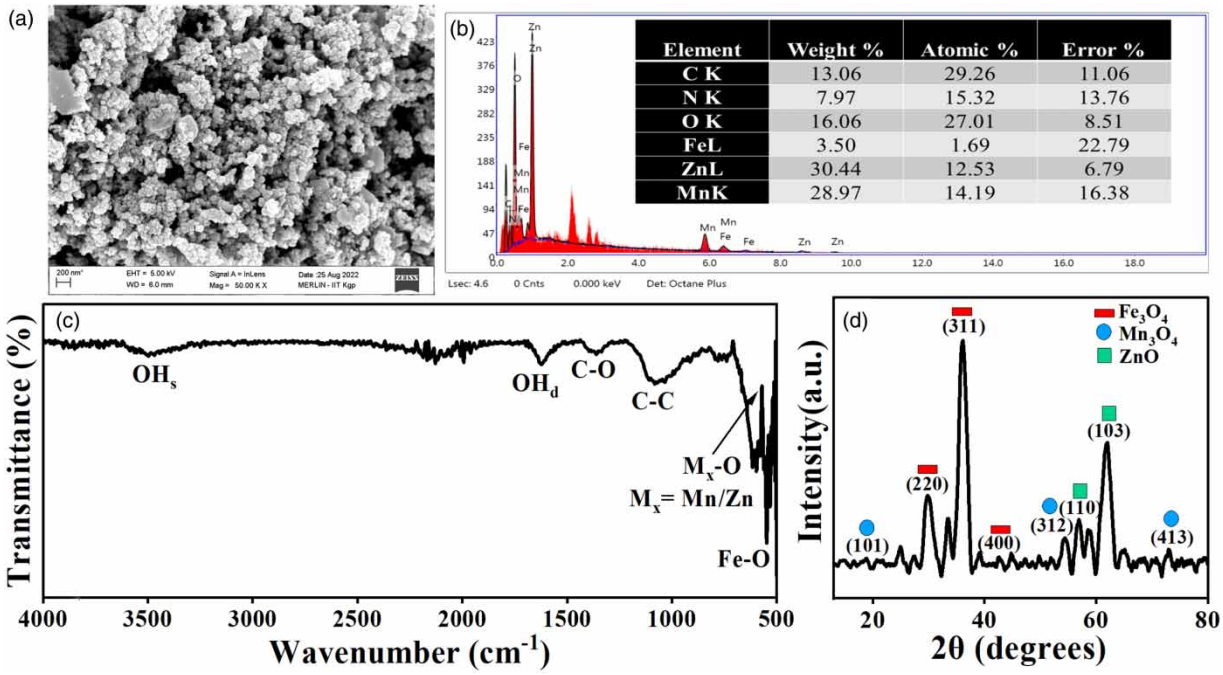

Figure 1 | (a) SEM image, (b) EDX, (c) FTIR, and (d) XRD of the catalyst prepared from battery waste.

Electrochemical characteristics of the catalyst

The electrochemical properties of the catalyst were assessed to explore the oxygen reduction reaction (ORR) activity of the catalyst. Figure 2(a) demonstrates the CV of the catalyst; clearly, a reduction peak was observed at a potential of about 0.35 V, corresponding to a CD of 10 mA/cm^2. However, the bare CF could only obtain a CD of 0.5 mA/cm^2 at a potential of 0.35 V. Therefore, an enhanced CV curve was obtained in the case of battery waste catalyst, which corroborates the high conductivity and redox properties of the as-synthesized electrocatalyst. These results were further justified by the LSV plots, which revealed a higher CD response in the case of electrocatalyst than the bare CF (Figure 2(b)). Besides, the Tafel curves were also explored, illustrating the overpotential of the catalyst required for ORR. A lower slope revealed an enhancement in the mass transfer efficiency of the catalyst; thus, a lower overpotential is required to attain faster ORR (Li *et al.* 2021). Figure 2(c) demonstrated a Tafel slope of 99 mV/dec for the Fe–Mn–Zn/C catalyst, which was 1.7 times lower than the slope of bare CF (169 mV/dec). Also, the corrosion potential of Fe–Mn–Zn/C was nearly –470 mV, which is more negative (lower) than the potential of CF (+ 9.0 mV). Hence, a lower corrosion potential reveals a lower resistance and a higher charge transfer ability, which was also illustrated in previous EF investigations (Ma *et al.* 2022). Thus, the battery waste catalyst might have higher ORR activity for reducing H_2O_2 into $^{\cdot}OH$. The EIS of the catalyst was also carried out with 50 mM Na_2SO_4; the semi-circular portion of the EIS plot signifies the charge transfer resistance of the electrocatalyst (Priyadarshini *et al.* 2023). Figure 2(d) showed a larger semicircle for CF ($Z' = 45\ \Omega$), which is nearly 10 Ω more than the Fe–Mn–Zn/C composites. Thereby, revealing an efficient charge transfer ability for faster ORR. Lastly, the stability of the catalyst was also depicted by performing 20 CV cycles. Figure 2(e) demonstrates only a 15.6% loss in absolute CD of the battery waste catalyst at a potential of about –2 V after 20 runs. Thus, revealing a high stability of electrocatalyst for the EF process.

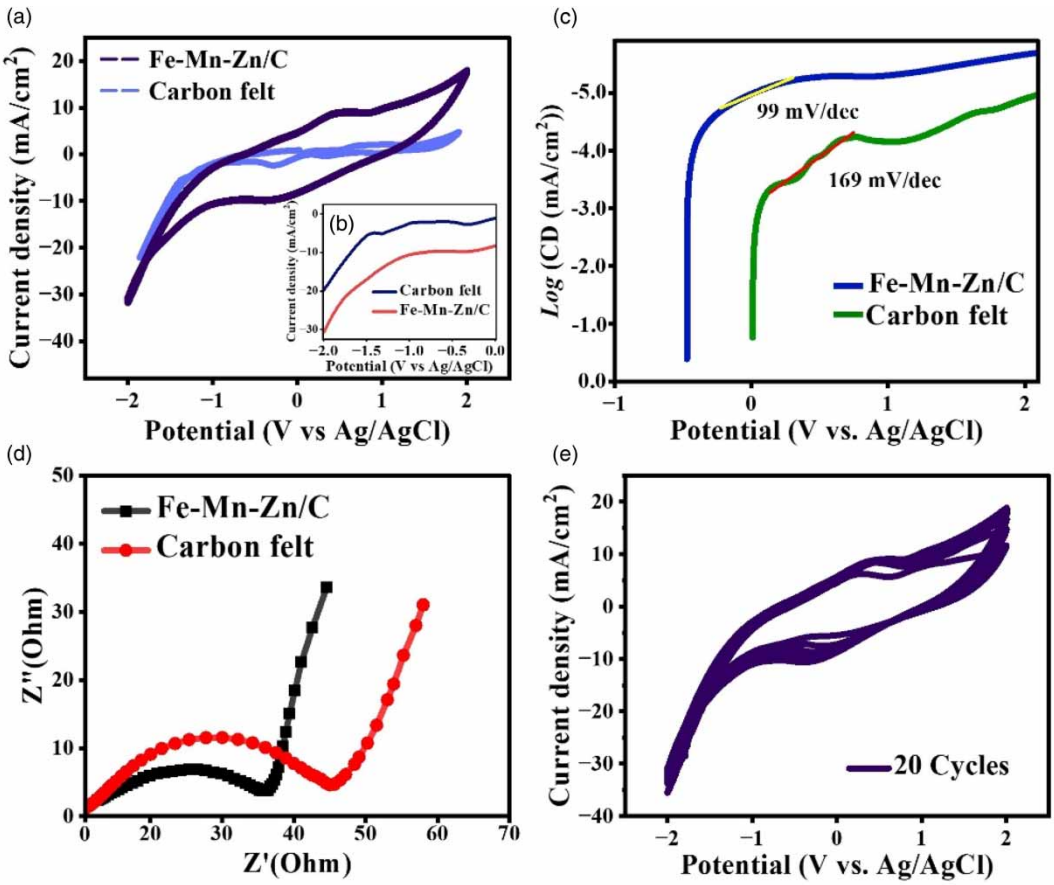

Figure 2 | (a) CV, (b) LSV, (c) Tafel slope, (d) EIS of CF and catalyst, and (e) 20 cycles of CV for analyzing the stability of synthesized catalyst ($Na_2SO_4 = 50$ mM and scan rate = 0.05 mV/s).

Performance of different systems for SDS removal

The performance efficacy of the as-synthesized electrocatalyst was explored in different systems to remove SDS. Three experiments, namely adsorption (without imposing external current), anodic oxidation (without catalyst), and EF (with catalyst), were executed under similar test conditions. The observation illustrated that after employing a CD of 5 mA/cm^2 at a pH of 7.2 for a retention time of 180 min, about 3.6 ± 1.1, 47.7 ± 3.1, and 83.9 ± 4.1% removal of 20 mg/L of SDS was obtained by adsorption (without external current), anodic oxidation, and EF process, respectively (Figure 3(a)). The higher removal in the case of EF might be ascribed to the *in-situ* formation of $^{\cdot}OH$ due to the reduction of H_2O_2 at the Fe–Mn–Zn/C-based cathode by 2e$^-$ reduction of oxygen molecule, which might cleave the sulfonic group of the SDS molecule and oxidize it into simpler molecular compounds; thereby, aiding SDS removal (Sathe *et al.* 2022).

In addition, the SDS removal kinetics model was explored at optimum operating conditions using Equations (3) and (4):

$$\ln\left(\frac{C_0}{C}\right) = k_1 t \tag{3}$$

$$\frac{1}{C} = \frac{1}{C_0} + k_2 t \tag{4}$$

where k_1 (min^{-1}) and k_2 (mg/L/min) are the apparent first and second-order rate constant, respectively. Also, C (mg/L), C_o (mg/L), and 't' are the SDS dosages at the final and initial electrolysis time (t), respectively.

After employing the optimum operating condition of CD of 5.0 mA/cm^2, Na_2SO_4 concentration of 0.05 M, initial pH of 7.2, initial SDS concentration of 20 mg/L, and electrolysis time of 180 min, k_1 and k_2 of 0.0095 min^{-1} and 0.0015 mg/L.min were

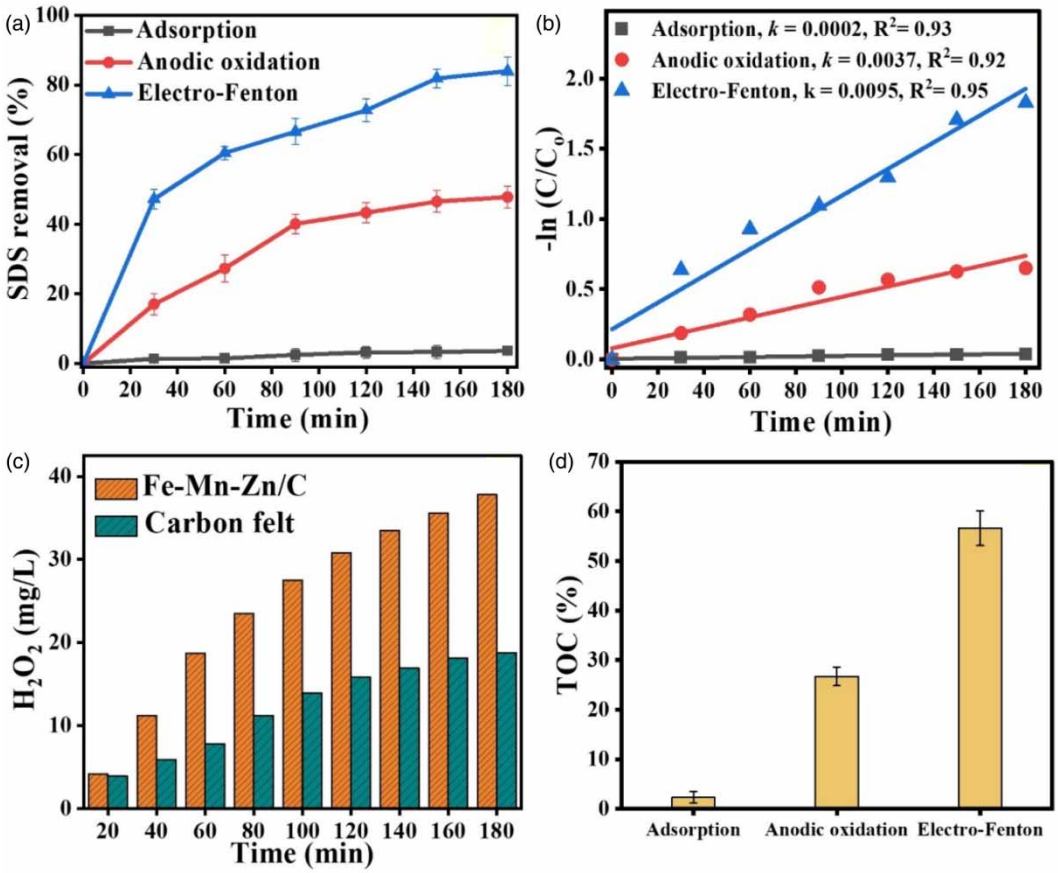

Figure 3 | (a) Removal of SDS (%) in different systems, (b) rate kinetics, (c) H_2O_2 production during EF process, and (d) TOC removal efficiency (pH = 7.2, Na_2SO_4 = 0.05 M, CD = 5.0 mA/cm^2, and SDS = 20 mg/L).

Table 1 | Kinetic model of the SDS removal in EF with Fe–Mn–Zn/C composites

Kinetic model	Equations used	Rate constants	Precision (R^2)
First order	$\ln(C_0/C) = k_1 t$	0.0095/min	0.983
Second order	$1/C = 1/C_0 + k_2 t$	0.0015 mg/L/min	0.947

obtained, respectively (Table 1). Moreover, a more precise linear relation was observed between ln (C_o/C) and time during the EF process, with a corresponding R^2 of 0.983 compared to $1/C - 1/C_o$ and time ($R^2 = 0.947$). Hence, the kinetic model during SDS removal followed pseudo-first-order kinetics. Similar trends were also observed by Ozcan and co-authors during the degradation of azinphos-methyl insecticide, wherein the degradation kinetics followed pseudo-first-order kinetics with rate constant of 0.41 min^{-1} (Özcan *et al.* 2013).

Among all the treatment processes, EF has the highest k value of 0.0095 min^{-1}, followed by anodic oxidation ($k = 0.0037$ min^{-1}) and adsorption ($k = 0.0002$ min^{-1}) (Figure 3(b)). These results are also justified by the production of H_2O_2 in the system. Figure 3(c) revealed nearly two times more H_2O_2 generation in Fe–Mn–Zn/C-based-EF process (37.8 mg/L) compared to control (CF without catalyst) (18.8 mg/L); as a result, a higher number of radical species were generated in the setup, leading to high removal in EF. Additionally, the mineralization of SDS in terms of TOC was explored, and about 2.3 ± 1.2, 26.7 ± 1.9, and 56.6 ± 3.5% removal of TOC were obtained after 180 min of treatment time via adsorption, anodic oxidation, and EF, respectively (Figure 3(d)). The degree of mineralization was lower compared to the abatement of SDS, which can be owing to the fact that the complete conversion of SDS into smaller end products like CO_2 and H_2O has not occurred, and intermediate by-products might be formed. Nonetheless, compared to adsorption and anodic oxidation, EF with battery waste catalyst has resulted in the comprehensive removal of SDS; hence, optimization of process parameters of EF was further carried out in subsequent sections.

Effect of CD

The efficacy of EF for SDS abatement is also governed by the CD, which is described as the imposed electrical current divided by the surface area of the electrode. Thus, a CD ranging between 3.4 and 5.8 mA/cm^2 was exerted between the electrodes to operate the EF for an optimum treatment time of 180 min at a pH of 7.2 and Na_2SO_4 dose of 0.05 M. Figure 4(a) disclosed that at a CD of 3.4, 4.2, 5.0, and 5.8 mA/cm^2, nearly 61.2 ± 3.8, 75.7 ± 3.5, 83.9 ± 4.1, and 85.7 ± 3.5% abatement of 20 mg/L of SDS, respectively, was obtained. Moreover, when the CD was increased from 3.4 to 5.8 mA/cm^2, the rate constants were also enhanced from 0.005 to 0.01 min^{-1} (Figure 4(b)). This can be due to the improved production of H_2O_2 at elevated CD; as a result, more reactive species are available for the degradation of SDS molecules (Yu *et al.* 2015). Thus, higher removal was achieved at higher CD. For example, when the CD was increased from 3.4 to 5.8 mA/cm^2, the H_2O_2 production was also amplified from 21.4 to 41.2 mg/L (Figure 4(c)). However, only 1.08-fold more H_2O_2 was produced at the CD of 5.8 mA/cm^2 compared to 5.0 mA/cm^2 due to the evolution of other side reactions, and only 1.8% more removal of SDS (85.7 ± 3.5%) was obtained at the CD of 5.8 mA/cm^2. Considering the above results, 5.0 mA/cm^2 was considered an optimal CD for further experimentation.

Effect of initial pollutant dose

The impact of initial SDS concentration is another crucial factor governing the performance of EF. In this regard, the efficacy of EF was evaluated by altering the SDS dose from 20 to 50 mg/L in the presence of 0.05 M Na_2SO_4 by employing a CD of 5.0 mA/cm^2 at a pH of 7.2 for 180 min of treatment time. At an initial SDS concentration of 20, 30, 40, and 50 mg/L, about 83.9 ± 4.1, 75.6 ± 2.7, 68.2 ± 3.2, and 61.7 ± 3.4% removal of SDS was achieved, respectively (Supplementary material, Figure S3). Moreover, when the dose of SDS was increased from 20 to 50 mg/L, the rate constant was also decreased from 0.0095 to 0.0052 min^{-1}, respectively (Figure 5(a)). The lower removal rate with an increase in pollutant dose can be due to the availability of lower $^{\cdot}OH$ for the degradation of a higher number of SDS (Daneshvar *et al.* 2008). Also, some intermediates formed during SDS degradation might continuously compete for their oxidation; as a result, they scavenge the $^{\cdot}OH$ species. Hence, the highest removal of SDS occurred at a concentration of 20 mg/L. Furthermore, SDS of concentration ranging between 3 and 20 mg/L is generally detected in municipal sewage (Saha *et al.* 2020). Therefore, in all other experiments, 20 mg/L is chosen as the optimum concentration.

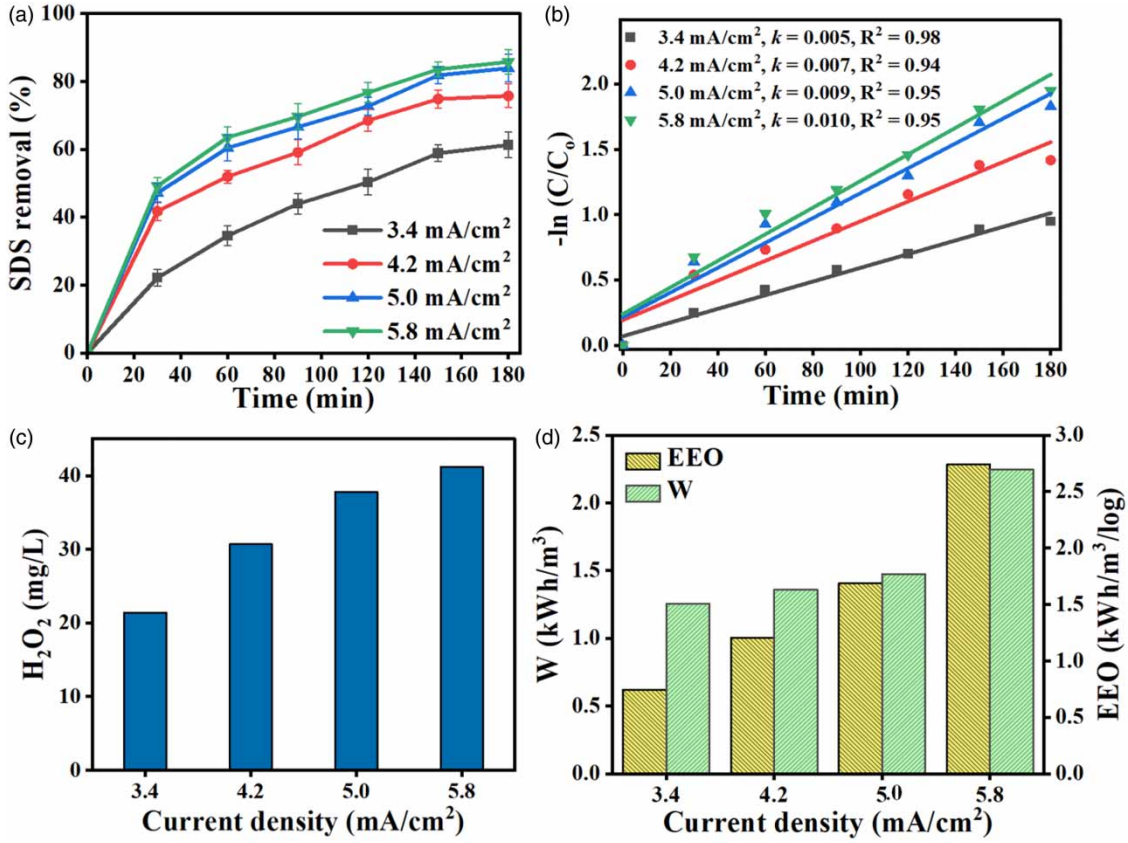

Figure 4 | (a) Effect of CD on SDS removal, (b) rate kinetics, (c) H_2O_2 production, and (d) energy consumption at different CD (pH = 7.2, Na_2SO_4 = 0.05 M, treatment time = 180 min, and SDS = 20 mg/L).

Effect of presence of anions

During the real-scale treatment of organic pollutants like SDS, the efficiency of EF might be affected due to the presence of inorganic anions, such as Cl^-, HCO_3^-, and NO_3^-. These ions compete with the reactive radicals present in the system for their removal; as a result, they scavenge the reactive species and can also alter them into less reactive radicals, thereby, decreasing the efficacy of EF, specifically the abatement of SDS. In this regard, the impact of Cl^-, HCO_3^-, and NO_3^- at concentrations of each ranging between 10 and 100 mM for 20 mg/L of SDS removal was explored. Supplementary material (Figure S3) revealed that with an increase in Cl^- from 10 to 100 mM, the SDS removal was decreased from about 87.9 ± 1.9 to 63.9 ± 2.3%; respectively, at an applied CD of 5.0 mA/cm^2 during 180 min of treatment time. Thus, the rate constants were initially increased from 0.009 to 0.010 min^{-1}, as the Cl^- concentration was increased from 0 to 10 mM (Figure 5(b)). The enhanced removal can be due to the formation of Cl_2/HOCl, which also oxidizes the SDS to some extent and aids in enhancing the removal rate (Aoudj *et al.* 2017). The positive effect of Cl^- on improving the efficiency of organic removal is in corroboration with the past reported investigations (Mandal *et al.* 2020). However, further enhancing the Cl^- concentration from 10 to 100 mM decreased the removal rate with a corresponding k value of about 0.008–0.005 min^{-1}, respectively (Figure 5(b)). The decline removal with an elevated chloride concentration can be due to the scavenging of $^{\bullet}OH$ owing to the presence of Cl^- in the setup (Quang *et al.* 2022).

On the other hand, when the concentration of each of HCO_3^- and NO_3^- ions was increased from 10 to 100 mM, the removal rate also declined from 0.0059 to 0.0031 min^{-1} for HCO_3^- and 0.0053 to 0.0025 min^{-1} for NO_3^- (Figure 5(c) and 5(d)). This can be ascribed to the formation of less reactive $CO_3^{\bullet -}$ and $NO_2^{\bullet}$ species due to the scavenging of $^{\bullet}OH$ by HCO_3^- and NO_2^-, respectively (Ghanbari *et al.* 2021). Hence, lower $^{\bullet}OH$ species were present for the degradation of SDS. Thus, in the presence of anions, the removal efficiency of SDS tends to decrease.

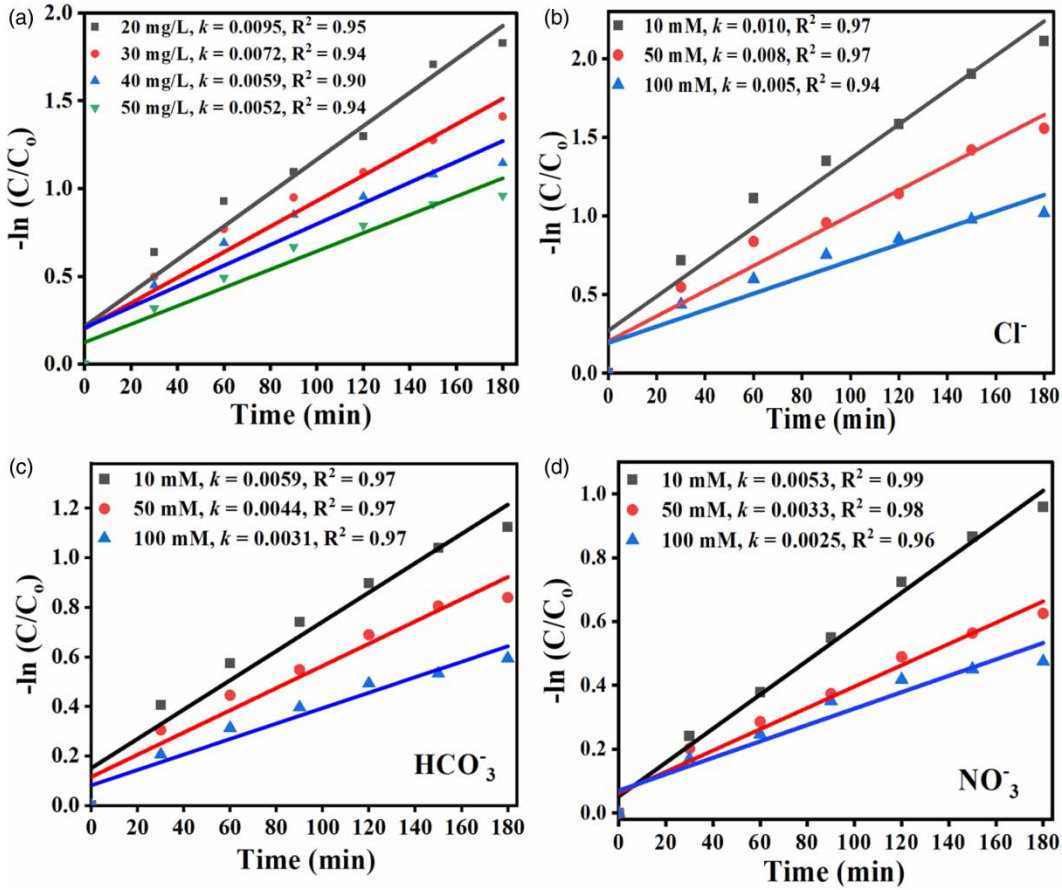

Figure 5 | (a) Effect of initial SDS concentration, (b) Cl^{-}, (c) HCO_3^{-}, and (d) NO_3^{-} on the removal of SDS (pH = 7.2, Na_2SO_4 = 0.05 M, treatment time = 180 min, SDS = 20 mg/L, the concentration of each ion ranged between 10 and 100 mM).

Reusability of the battery waste-coated cathode

To determine the feasibility of the as-synthesized catalyst for the real-scale application of wastewater treatment via EF, the performance of Fe–Mn–Zn/C composite catalyst-based cathode electrode was explored for six consecutive cycles without any regeneration process. Figure 6(a) revealed that after six consecutive cycles, only 4.6% lower removal of SDS (79.6%) was obtained compared to the initial cycle (83.9%), thereby validating reasonable durability and reusability of the Fe–Mn–Zn/C composites. However, declined removal efficiency can be ascribed to the blockage of the activation sites of the catalyst to produce reactive radical species owing to the adsorption of organic molecules on the surface area of the electrodes. Therefore, treatments like rinsing the cathode with ethanol or water after a few successive cycles can possibly recover the active sites of the cathode, which would be beneficial for field-scale applications of the EF process. In addition, the leaching of Fe, Mn, and Zn from the composites was also evaluated during the six runs. The observations disclosed that after 180 min of reaction time, nearly 0.45 mg/L of Fe, 0.15 mg/L of Mn, and 0.27 mg/L of Zn were leached out from the composites. The final leaching concentration in the solution is within the permissible limit of Indian wastewater discharge units (Sawal 1986). Moreover, the concentration of Fe in the effluent was also within the European discharge permissible limit of wastewater (Fernández-Sáez *et al.* 2019).

Besides, the feasibility of Fe–Mn–Zn/C composites was also investigated for the treatment of real wastewater containing SDS. In this context, about 16.5 ± 0.8 mg/L of SDS was spiked in secondary treated municipal sewage (already containing about 3.3 ± 0.3 mg/L of SDS) to achieve a total SDS concentration of nearly 20 mg/L in treated sewage. After employing optimum EF conditions for 180 min, about 72.2 ± 2.7% removal of SDS was obtained (Figure 6(b)). Thus, around 11.7% lower removal of SDS was obtained in real wastewater compared to synthetic wastewater. The reduced removal can be due to the presence of other competing organic pollutants in the wastewater, which scavenge the reactive radicals for

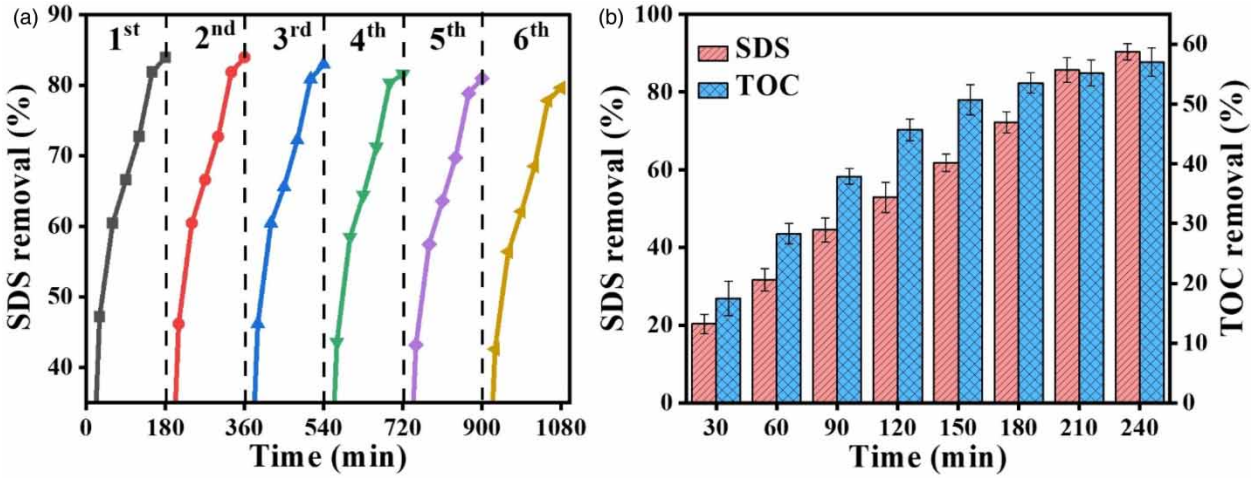

Figure 6 | (a) SDS removal during six consecutive cycles and (b) performance of EF in real wastewater in terms of SDS and TOC abatement.

their removal (Malakootian *et al.* 2019). Therefore, lower radicals were available to abate SDS, which declined the removal efficiency of SDS in real wastewater.

Nonetheless, to achieve the reasonable remediation of about 20 mg/L of SDS in wastewater, prolonged EF of an additional 60 min was carried out, keeping all other conditions at optimum. The result revealed around 90.3 ± 2.1% reduction of SDS, which suggests the significant performance of battery waste-based catalyst in EF for the real-scale wastewater treatment application (Figure 6(b)). Additionally, about 57 ± 2.6% of TOC removal was also obtained with an initial TOC of 30.2 ± 2.8 mg/L after externally adding SDS (TOC of about 11.3 ± 1.2 mg/L for 16.5 ± 0.8 mg/L of SDS and TOC present in treated sewage of 18.9 ± 2.4 mg/L) at a wastewater pH of 7.2 during 240 min of treatment time with an applied CD of 5.0 mA/cm^2 (Figure 6(b)).

Identification of the contribution of free radicals in SDS degradation

In general, both $O_2^{\bullet-}$ and $^{\bullet}OH$ participate in the degradation of SDS in the EF process. Thus, to identify the major contribution of reactive oxidative species (ROS) responsible for SDS degradation in the EF process, active species capturing experiments were conducted, where TBA and EtOH for $^{\bullet}OH$, BQ for $O_2^{\bullet-}$ with varying concentrations of 10, 50, and 100 mM were added to the solution (Zhou *et al.* 2021). The experiment findings demonstrated that adding 10–100 mM of BQ, EtOH, and TBA to the EF system significantly decreased the SDS degradation efficiency from 83.9 ± 4.1 to 78.5 ± 3.8%, 83.9 ± 4.1 to 59.4 ± 2.5%, and 83.9 ± 4.1 to 62.8 ± 3.2%, respectively (Supplementary material, Table S1). The decrease in degradation efficiency with increased dosages of EtOH and TBA confirmed that the $^{\bullet}OH$ present was effectively scavenged and played a dominant role in the degradation of SDS compared to $O_2^{\bullet-}$ in the EF process. Moreover, to confirm the electrochemical production of H_2O_2 in the EF system, catalase (CAT), an H_2O_2 scavenger, was added to the system. The results demonstrated that in the presence of 2,000 U/mL of CAT, the SDS degradation efficiency decreased from 83.9 ± 4.1% to 34.5 ± 5.8%, revealing that the H_2O_2 was the main species responsible for the formation of $^{\bullet}OH$ in the EF system (Equation (2)).

In addition, EPR experimentation was performed using the trapping agent DMPO, with DMPO – $^{\bullet}O_2^-$ (methanol dispersion) and DMPO – $^{\bullet}OH$ (aqueous dispersion) to confirm the generation of $^{\bullet}O_2^-$ and $^{\bullet}OH$ in the system, respectively. The result revealed strong characteristic peaks of DMPO – $^{\bullet}OH$ with an intensity ratio of four waves as 1:2:2:1 in the presence of Fe–Mn–Zn/C in the EF system, suggesting the presence of metals in catalyst-activated H_2O_2 to generate $^{\bullet}OH$ (Supplementary material, Figure S4). However, no symmetric peak was observed in the DMPO – $^{\bullet}O_2^-$ adduct. Thus, the quenching experiments and EPR results suggested that the $^{\bullet}OH$ was the dominant species generated with Fe–Mn–Zn/C through the 2e$^-$ route oxygen reduction. The aforementioned finding was consistent with the earlier investigation, in which a major contribution of $^{\bullet}OH$ was seen in the hetero-EF degradation of bisphenol A using a Co/Fe_3O_4@PZS modified cathode (Zhou *et al.* 2021).

Degradation mechanism and pathway of SDS

The waste battery-based Fenton catalyst reduces the H_2O_2 to generate $^{\cdot}OH$ species, which is beneficial for the degradation of SDS molecules. The $^{\cdot}OH$ attacks the hydrophilic SO_4Na group of the SDS owing to its polar nature; thereby cleaving it (Sathe *et al.* 2022). The oxidized product of SDS is further oxidized to an aldehyde and do-decanoic acid. Therefore, in the current exploration, the possible degradation pathway of SDS is by the production of dodecanol. The dodecanol was oxidized via $^{\cdot}OH$ to convert dodecanal, which was further oxidized to decanoic acid, which is commonly known as lauric acid.

The MALDI-TOF disclosed the existence of SDS ($m/z = 273.44$) in the influent, which was detected with reduced intensity in the effluent, revealing the effective removal of SDS in the EF system (Figure 7(a) and 7(b)) (Saha *et al.* 2020). Moreover, a peak at 199.41 (Figure 7(b)) signifies the formation of lauric acid as an intermediate product during the mineralization of the SDS molecule, which was also reported in previous works (Sathe *et al.* 2022). The intermediate lauric acid is not a recalcitrant product and can be further degraded by applying low-cost biological technologies or prolonging the reaction time in the same setup.

Economic assessment

The economic analysis was carried out to assist the viability of the EF technology based on the operating cost (OC_{total}) required to remove SDS by one order of magnitude for one m^3 of SDS-laden wastewater, which is also termed as OC_{total} per order. The OC_{total} is comprised of catalyst cost, chemical cost, and electricity cost, which was evaluated by estimating the energy consumption (W) and electrical energy per order (EEO) as per Equations (5)–(9) (Priyadarshini *et al.* 2023):

$$W(\text{kWh/m}^3) = \frac{\text{UIT}}{V} \tag{5}$$

$$\text{EEO}\left(\frac{\text{kWh/m}^3}{\log}\right) = \frac{W}{\log(C_o/C)} \tag{6}$$

$$\text{OC}_{\text{total}} = \text{Catalyst cost} + \text{Chemical cost} + \text{Electricity cost} \tag{7}$$

where U is the voltage (V), I is the imposed current (A), T is the treatment time (h), V is the working volume (m^3), C_o and C are initial and final concentrations of SDS (mg/L), respectively.

$$\text{Chemical cost } (\$/\text{m}^3) = \text{Electrolyte consumption } (\text{kg/m}^3) \times \text{cost of electrolyte } (\$/\text{kg}) \tag{8}$$

$$\text{Electricity cost } (\$/\text{m}^3) = \text{EEO } (\text{kWh/m}^3/\text{log}) \times \text{per unit cost of electricity } (\$/\text{kWh}) \tag{9}$$

After employing the optimum operating condition of 0.05 M of Na_2SO_4, CD of 5.0 mA/cm^2, pH of 7.2, and initial SDS dose of 20 mg/L, the battery waste-based-EF process consumes electricity cost, electrolyte cost, and catalyst cost of around 0.176, 0.170, and 0.01 \$/m^3, respectively (Table 2). Hence, the total operating cost (OC_{total}) of nearly 0.35 US\$ (or 28.70 ₹) is

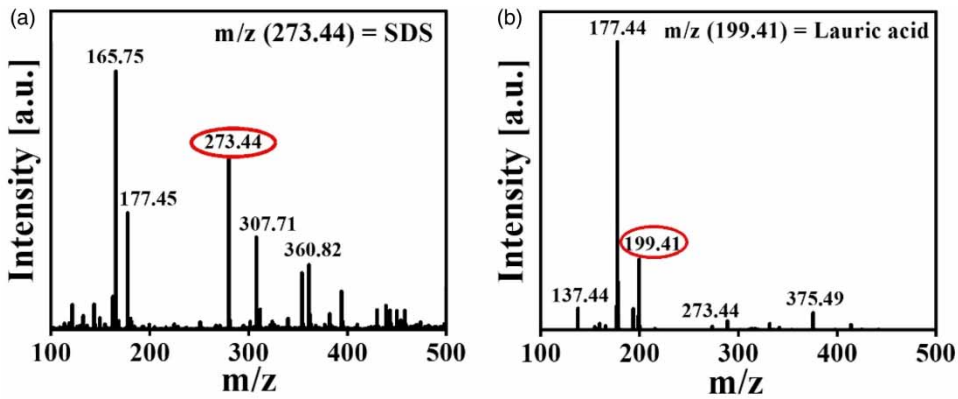

Figure 7 | MALDI – TOF: (a) initial SDS influent and (b) EF treated effluent (pH = 7.2, Na_2SO_4 = 0.05 M, treatment time = 180 min, SDS = 20 mg/L).

Table 2 | Economic analysis of the battery waste-based-EF process for SDS abatement

Parameter	Value
k (min^{-1})	0.0095
W (kWh/m^3)	1.40
EEO (kWh/m^3/log)	1.76
Electricity cost ($/$m^3$)	0.176
Electrolyte cost ($/$m^3$)	0.170
Catalyst cost ($/$m^3$)	0.01
OC_{total} ($/$m^3$)	0.35

Note: All pricing is based on commercial cost; per unit (kWh) cost of electricity = 0.1 $, per kg cost of sodium sulfate = 0.024 $, per liter cost of HCl = 0.043 $, per kg cost of NH_4OH salt = 0.22 $.

required to treat per m^3 of SDS wastewater. Besides, a cost comparison of other existing technologies for SDS removal is summarized in Supplementary material, Table S2.

Additionally, it was also observed that amplifying the CD also increases the energy consumption of the EF process, which is evaluated by calculating the W and EEO at distinct CDs. Figure 4(d) (section: effect of CD) revealed that as the CD was increased from 5.0 to 5.8 mA/cm^2, the W and EEO were also increased from 1.5 to 2.28 kWh/m^3 and 1.75 to 2.69 kWh/m^3-log, respectively.

CONCLUSION

The current investigation demonstrates a waste-to-treat-waste approach by synthesizing and applying battery waste-based electrocatalysts in the EF process to treat SDS-laden wastewater effectively. The magnetic Fe–Mn–Zn/C composites utilized in EF resulted in about 83.9 ± 4.1% removal of 20 mg/L of SDS at an optimum CD of 5.0 mA/cm^2, Na_2SO_4 dose of 0.05 M during 180 min of treatment time. The EF process outperformed the adsorption and anodic oxidation process for SDS removal. Chloride ions at a concentration of 10 mM have a positive effect on SDS removal. However, nitrate and carbonate ions at a concentration ranging between 10 and 100 mM inhibit the removal efficiency of EF for SDS abatement. Moreover, an operating cost of about 0.35 $ per m^3 per order was required to treat SDS wastewater. The catalyst also demonstrated high recyclability and low iron leaching up to six cycles of EF.

Furthermore, 1.33-fold more treatment time is required for efficacious removal of SDS (about 90%) in secondary treated real wastewater compared to synthetic wastewater. Additionally, about 57.0 ± 2.6% of TOC removal was also obtained with the battery waste-based-EF process. The Fe–Mn–Zn/C-based CF cathode system produced higher amount of H_2O_2, which was activated to generate $^{\cdot}OH$ radicals through the metals present in the as-synthesized catalyst. However, nearly 2-fold lower H_2O_2 was formed on the cathode without catalyst (control), which suggested that the battery waste catalyst enhances the electrocatalytic activity of the cathode for efficacious Fenton oxidation of SDS surfactant. Thus, Fe–Mn–Zn/C composites are a novel waste-derived catalyst that is simply synthesized for its effective application in EF. However, future investigations can be further carried out for its utilization as an electrocatalyst in other technologies.

ACKNOWLEDGEMENT

The Department of Science and Technology, Government of India, is thanked by the authors for supporting this research project financially (File No. DST/TMD (EWO)/OWUIS-2018/RS-10).

AUTHORS CONTRIBUTIONS

A.A. was involved in conceptualization; formal analysis; investigation; methodology; roles/writing – original draft; writing – review and editing; M.P. was involved in validation; visualization; roles/writing – original draft; data curation; writing – review and editing; investigation; M.M.G. was involved in funding acquisition; project administration; resources; supervision; validation; writing – review and editing. R.Y.S. was involved in supervision; validation; writing – review and editing.

DISCLOSURE STATEMENT

The authors state that they are aware of no personal or financial conflicts that would affect the research project described in this exploration.

FUNDING

The Department of Science and Technology, Government of India, provided funding assistance for this research project (File No. DST/TMD (EWO)/OWUIS-2018/RS-10).

DATA AVAILABILITY STATEMENT

Data cannot be made publicly available; readers should contact the corresponding author for details.

CONFLICT OF INTEREST

The authors declare there is no conflict.

REFERENCES

Aoudj, S., Khelifa, A. & Drouiche, N. 2017 Removal of fluoride, SDS, ammonia and turbidity from semiconductor wastewater by combined electrocoagulation–electroflotation. *Chemosphere* **180**, 379–387. https://doi.org/10.1016/j.chemosphere.2017.04.045.

Arun, J., Gopinath, K. P., Vo, D. V. N., SundarRajan, P. S. & Swathi, M. 2020 Co-hydrothermal gasification of Scenedesmus sp. with sewage sludge for bio-hydrogen production using novel solid catalyst derived from carbon-zinc battery waste. *Bioresource Technology Reports* **11** (May), 100459. https://doi.org/10.1016/j.biteb.2020.100459.

Bashir, A. K. H., Mayedwa, N., Kaviyarasu, K., Razanamahandry, L. C., Matinise, N., Bharuth-Ram, K., Tchokonté, M. B. T., Ezema, F. I. & Maaza, M. 2019 Investigation of electrochemical performance of the biosynthesized α-Fe_2O_3 nanorods. *Surfaces and Interfaces* **17** (June), 100345. https://doi.org/10.1016/j.surfin.2019.100345.

Chen, X., Li, J., Kang, D., Zhou, T. & Ma, H. 2019 A novel closed-loop process for the simultaneous recovery of valuable metals and iron from a mixed type of spent lithium-ion batteries. *Green Chemistry* **21** (23), 6342–6352. https://doi.org/10.1039/c9gc02844g.

Daneshvar, N., Aber, S., Vatanpour, V. & Rasoulifard, M. H. 2008 Electro-Fenton treatment of dye solution containing Orange II: Influence of operational parameters. *Journal of Electroanalytical Chemistry* **615** (2), 165–174. https://doi.org/10.1016/j.jelechem.2007.12.005.

Fernández-Sáez, N., Villela-Martinez, D. E., Carrasco-Marín, F., Pérez-Cadenas, A. F. & Pastrana-Martínez, L. M. 2019 Heteroatom-doped graphene aerogels and carbon-magnetite catalysts for the heterogeneous electro-Fenton degradation of Acetaminophen in aqueous solution. *Journal of Catalysis* **378**, 68–79. https://doi.org/10.1016/j.jcat.2019.08.020.

Fu, T., Gong, X., Guo, J., Yang, Z. & Liu, Y. 2021 Zn-CNTs-Cu catalytic in-situ generation of H_2O_2 for efficient catalytic wet peroxide oxidation of high-concentration 4-chlorophenol. *Journal of Hazardous Materials* **401** (April 2020), 123392. https://doi.org/10.1016/j.jhazmat.2020.123392.

Gan, Q., Hou, H., Liang, S., Qiu, J., Tao, S., Yang, L., Yu, W., Xiao, K., Liu, B., Hu, J., Wang, Y. & Yang, J. 2020 Sludge-derived biochar with multivalent iron as an efficient Fenton catalyst for degradation of 4-Chlorophenol. *Science of the Total Environment* **725**, 138299. https://doi.org/10.1016/j.scitotenv.2020.138299.

Ghanbari, F., Hassani, A., Wacławek, S., Wang, Z., Matyszczak, G., Lin, K. Y. A. & Dolatabadi, M. 2021 Insights into paracetamol degradation in aqueous solutions by ultrasound-assisted heterogeneous electro-Fenton process: Key operating parameters, mineralization and toxicity assessment. *Separation and Purification Technology* **266** (February), 118533. https://doi.org/10.1016/j.seppur.2021.118533.

Graf, E. & Penniston, J. T. 1980 Method for determination of hydrogen peroxide, with its application illustrated by glucose assay. *Clinical Chemistry* **26** (5), 658–660. https://doi.org/10.1093/clinchem/26.5.658.

Li, X., Xiao, C., Ruan, X., Hu, Y., Zhang, C., Cheng, J. & Chen, Y. 2021 Enrofloxacin degradation in a heterogeneous electro-Fenton system using a tri-metal-carbon nanofibers composite cathode. *Chemical Engineering Journal* **427** (March 2021), 130927. https://doi.org/10.1016/j.cej.2021.130927.

Loudiki, A., Matrouf, M., Azriouil, M., Laghrib, F., Farahi, A., Bakasse, M., Lahrich, S. & El Mhammedi, M. A. 2022 Graphene oxide synthesized from zinc-carbon battery waste using a new oxidation process assisted sonication: Electrochemical properties. *Materials Chemistry and Physics* **275** (July 2021), 125308. https://doi.org/10.1016/j.matchemphys.2021.125308.

Ma, X., Rao, T., Zhao, M., Jia, Z., Ren, G., Liu, J., Guo, H., Wu, Z. & Xie, H. 2022 A novel induced zero-valent iron electrode for in-situ slow release of Fe2 + to effectively trigger electro-Fenton oxidation under neutral pH condition: Advantages and mechanisms. *Separation and Purification Technology* **283** (September 2021), 120160. https://doi.org/10.1016/j.seppur.2021.120160.

Malakootian, M., Kannan, K., Gharaghani, M. A., Dehdarirad, A., Nasiri, A., Shahamat, Y. D. & Mahdizadeh, H. 2019 Removal of metronidazole from wastewater by Fe/charcoal micro electrolysis fluidized bed reactor. *Journal of Environmental Chemical Engineering* **7** (6), 103457. https://doi.org/10.1016/j.jece.2019.103457.

Mandal, P., Gupta, A. K. & Dubey, B. K. 2020 Role of inorganic anions on the performance of landfill leachate treatment by electrochemical oxidation using graphite/pbo2 electrode. *Journal of Water Process Engineering* **33** (June 2019), 101119. https://doi.org/10.1016/j.jwpe.2019.101119.

Mondal, B., Adak, A. & Datta, P. 2019 Degradation of anionic surfactant in municipal wastewater by UV-H_2O_2 : process optimization using response surface methodology. *Journal of Photochemistry and Photobiology A: Chemistry* 237–243. https://doi.org/10.1016/j.jphotochem.2019.02.030.

Naseem, T., Zain-ul-Abdin, Waseem, M., Hafeez, M., Din, S. U., Haq, S. & Mahfoz-ur-Rehman 2020 Reduced graphene oxide/Zinc oxide nanocomposite: from synthesis to its application for wastewater purification and antibacterial activity. *Journal of Inorganic and Organometallic Polymers and Materials* **30** (10), 3907–3919. https://doi.org/10.1007/s10904-020-01529-2.

Özcan, A., Şahin, Y. & Oturan, M. A. 2013 Complete removal of the insecticide azinphos-methyl from water by the electro-Fenton method – A kinetic and mechanistic study. *Water Research* **47** (3), 1470–1479. https://doi.org/10.1016/j.watres.2012.12.016.

Ozturk, D. 2022 Fe_3O_4/Mn_3O_4/ZnO-rGO hybrid quaternary nano-catalyst for effective treatment of tannery wastewater with the heterogeneous electro-Fenton process: Process optimization. *Science of the Total Environment* **828**, 154473. https://doi.org/10.1016/j.scitotenv.2022.154473.

Priyadarshini, M., Ahmad, A., Das, S. & Ghangrekar, M. M. 2022 Application of innovative electrochemical and microbial electrochemical technologies for the efficacious removal of emerging contaminants from wastewater: A review. *Journal of Environmental Chemical Engineering* **10** (5), 108230. https://doi.org/10.1016/j.jece.2022.108230.

Priyadarshini, M., Ahmad, A. & Ghangrekar, M. M. 2023 Efficient upcycling of iron scrap and waste polyethylene terephthalate plastic into Fe_3 O_4@ C incorporated MIL-53 (Fe) as a novel electro-Fenton catalyst for the degradation of salicylic acid ⋆. *Environmental Pollution* **322** (January), 121242. https://doi.org/10.1016/j.envpol.2023.121242.

Qi, H., Sun, X. & Sun, Z. 2022 Cu-doped Fe_2O_3 nanoparticles/etched graphite felt as bifunctional cathode for efficient degradation of sulfamethoxazole in the heterogeneous electro-Fenton process. *Chemical Engineering Journal* **427** (May 2021), 131695. https://doi.org/10.1016/j.cej.2021.131695.

Quang, H. H. P., Din, N. T., Thi, T. N. T., Bao, L. T. N., Yuvakkumar, R. & Nguyen, V.-H. 2022 Fe2 + , Fe3 + , Co2 + as highly efficient cocatalysts in the homogeneous electro-Fenton process for enhanced treatment of real pharmaceutical wastewater. *Journal of Water Process Engineering* **46** (December 2021), 102635. https://doi.org/10.1016/j.jwpe.2022.102635.

Saha, J., Chakraborty, I. & Ghangrekar, M. M. 2020 A novel tin-chloride-zirconium oxide-kaolin composite coated carbon felt anode for electro-oxidation of surfactant from municipal wastewater. *Journal of Environmental Chemical Engineering* **8** (6), 104489. https://doi.org/10.1016/j.jece.2020.104489.

Sathe, S. M., Chakraborty, I., Doki, M. M., Dubey, B. K. & Ghangrekar, M. M. 2022 Waste-derived iron catalyzed bio-electro-Fenton process for the cathodic degradation of surfactants. *Environmental Research* **212** (PA), 113141. https://doi.org/10.1016/j.envres.2022.113141.

Sawal, M. 1986 General standards for discharge of environmental pollutants. *The Environment (Protection) Rules* **2** (174), 545–560.

Setiadi, E. A., Priyadi, I., Siregar, E. M., Tetuko, A. P., Kurniawan, C., Achiruddin & Sebayang, P. 2019 The effect of NH_4OH pH on the synthesis of mnfe2o4 as heavy metal adsorbent by using co-precipitation method. *Journal of Physics: Conference Series* **1191** (1), 012040. https://doi.org/10.1088/1742-6596/1191/1/012040.

Shi, L., Li, N., Wang, C. & Wang, C. 2010 Catalytic oxidation and spectroscopic analysis of simulated wastewater containing o-chlorophenol by using chlorine dioxide as oxidant. *Journal of Hazardous Materials* **178** (1–3), 1137–1140. https://doi.org/10.1016/j.jhazmat.2010.01.125.

Subramani, K. & Sathish, M. 2019 Facile synthesis of ZnO nanoflowers/reduced graphene oxide nanocomposite using zinc hexacyanoferrate for supercapacitor applications. *Materials Letters* **236**, 424–427. https://doi.org/10.1016/j.matlet.2018.10.111.

Wu, M., Song, S., Wang, T., Sun, W., Xu, S. & Yang, Y. 2022 Natural sphalerite photocatalyst for treatment of oily wastewater produced by solvent extraction from spent lithium-ion battery recycling. *Applied Catalysis B: Environmental* **313** (March), 121460. https://doi.org/10.1016/j.apcatb.2022.121460.

Yang, F., Hu, X., Gao, S., Liu, X., Zhou, S. & Kong, Y. 2020 Enabling synchronous activation of inner-core and mesoporous outer-shell of monodispersed Fe_3O_4@SiO_2 by in-situ implanted MnOx to synergistically deliver enhanced catalytic activity. *Journal of Alloys and Compounds* **842**, 155817. https://doi.org/10.1016/j.jallcom.2020.155817.

Ye, M., Zhang, C., Liu, Z., Li, H., Fu, Z., Zhang, H., Wang, G. & Zhang, Y. 2023 E-waste derived CuAu bimetallic catalysts supported on carbon cloth enabling effective degradation of bisphenol A via an electro-Fenton process. *Separation and Purification Technology* **305** (November 2022), 122507. https://doi.org/10.1016/j.seppur.2022.122507.

Yu, F., Zhou, M. & Yu, X. 2015 Cost-effective electro-Fenton using modified graphite felt that dramatically enhanced on H_2O_2 electro-generation without external aeration. *Electrochimica Acta* **163**, 182–189. https://doi.org/10.1016/j.electacta.2015.02.166.

Yüksel, E., Şengil, I. A. & Özacar, M. 2009 The removal of sodium dodecyl sulfate in synthetic wastewater by peroxi-electrocoagulation method. *Chemical Engineering Journal* **152** (2–3), 347–353. https://doi.org/10.1016/j.cej.2009.04.058.

Zavar, S. 2017 A novel three component synthesis of 2-amino-4H-chromenes derivatives using nano ZnO catalyst. *Arabian Journal of Chemistry* **10**, S67–S70. https://doi.org/10.1016/j.arabjc.2012.07.011.

Zhou, H., Dong, H., Wang, J. & Chen, Y. 2021 Cobalt anchored on porous N, P, S-doping core-shell with generating/activating dual reaction sites in heterogeneous electro-Fenton process. *Chemical Engineering Journal* **406**, 125990. https://doi.org/10.1016/j.cej.2020.125990.

First received 14 July 2023; accepted in revised form 10 January 2024. Available online 5 February 2024